Phosphorylation of STAT3 Serine-727 by Cyclin-Dependent Kinase 1 Is Critical for Nocodazole-Induced Mitotic Arrest†

Xiaoqing Shi,‡ Hong Zhang,§ Harry Paddon,‡ Gloria Lee,§ Xinmin Cao,|| and Steven Pelech*,‡,§

Brain Research Center and Department of Medicine, University of British Columbia, Vancouver, Canada, Kinexus Bioinformatics Corporation, Vancouver, Canada, and Signal Transduction Laboratory, Institute of Molecular and Cell Biology, Singapore, Republic of Singapore

Received December 6, 2005; Revised Manuscript Received March 8, 2006

ABSTRACT: Signal transducer and activator of transcription 3 (STAT3) mediates cellular responses to diverse cytokines and growth factors by modulating the expression of specific target genes. While phosphorylation of STAT3 at Tyr-705 has been demonstrated to be a prerequisite for STAT3 dimerization, nuclear translocation, and activation of gene transcription, the role of Ser-727 in regulation of STAT3 activity is controversial. Kinetworks KPSS-1.1 phospho-site screening of nocodazole-treated HeLa cells revealed that STAT3 Ser-727 phosphorylation was enhanced during mitosis, and this correlated with a reduction of Tyr-705 phosphorylation. Overexpression of STAT3 mutants in which these phosphorylation sites were separately abolished revealed that phosphorylation at these sites appeared to be mutually antagonistic. The nocodazole-induced STAT3 Ser-727 phosphorylation was reduced by selective inhibition of CDK1 phosphotransferase activity, and CDK1 could directly phosphorylate GST-STAT3 Ser-727 in vitro and co-immunoprecipitate with STAT3 in vivo. Blocking Ser-727 phosphorylation enhanced STAT3 DNA-binding activity toward its target gene promoters, implying a negative effect of Ser-727 phosphorylation on its transcriptional activity. Interference of Ser-727 phosphorylation resulted in an exit from mitotic arrest induced by nocodazole treatment and a cell cycle arrest at the G1 phase, as indicated by the accumulation of 2N cell population and enhanced expression of G1 cell cycle regulators including $p21^{CIP1/WAF1}$, $p27^{Kip1}$, and cyclin E. Taken together, our observations point to a novel role of STAT3 Ser-727 phosphorylation in control of the onset and maintenance of the M phase during the cell cycle through downregulation of CDK inhibitors.

STAT3[1] belongs to a family of signal transducing transcription factors that play critical roles in mediating cellular responses to diverse cytokines and growth factors by modulation of the expression of specific target genes (*1, 2*). Engagement of cytokines and growth factors to their cognate receptors induces STAT3 Tyr-705 (Y705) phosphorylation either by receptor-associated tyrosine kinases in the Janus kinase (JAK) and Src kinase families or by intrinsic receptor-tyrosine kinases such as epidermal growth factor receptor (EGFR), leading to STAT3 dimerization through reciprocal phosphotyrosine-SH2 domain interactions, nuclear translocation, and binding to enhancer/promoter sequences of target genes (*3, 4*).

Since constitutive activation of STAT3 is found in a wide variety of malignancies including cancers (*5*−*7*), the mechanism underlying the activation of STATs has been the focus of extensive studies in recent years. While the tyrosine phosphorylation of STATs mediated by nonreceptor and receptor-tyrosine kinases seems to be the paradigm for STAT activation utilized by a large number of cytokines and growth factors, recent studies have provided substantial evidence for the phosphorylation of a serine residue within the COOH-terminal transcriptional activation domain of most of the STATs (*8*−*10*). The serine residue is located within a conserved PMSP (or PSP) motif among STAT1, -3, -4, and -5, but not STAT2 and -6, and corresponds to serine-727 (S727) in STAT3 (*9, 11, 12*). It has been demonstrated that mitogen-activated protein kinases (MAPKs), protein kinase C-delta isoform (PKCδ), the mammalian target of rapamycin kinase (mTOR), and protein kinase R (PKR) mediate serine phosphorylation either directly or indirectly in a stimulus or cell type dependent manner (*13*−*18*), indicating that STATs may be convergent points for integration of signals from multiple pathways. In contrast to the well-characterized role for activation of STATs by tyrosine phosphorylation, the effect of serine phosphorylation on STAT DNA-binding/transcriptional activity has been controversial. While some evidence supports a positive role for S727 phosphorylation in STAT3 transcriptional activation, presumably through enhanced recruitment of transcriptional cofactors, there is also emerging evidence for a negative role for serine phosphorylation, although the exact underlying mechanism is unclear (*11, 19*).

† This work is supported by a research grant from the Canadian Institute of Health Research to S.P.

* To whom correspondence should be addressed. Tel: 604-822-9966. Fax: 604-822-9963. E-mail: spelech@kinexus.ca.

‡ University of British Columbia.

§ Kinexus Bioinformatics Corporation.

|| Institute of Molecular and Cell Biology.

[1] Abbreviations: BrdU, 5-bromo-2-deoxyuridine; CDK, cyclin-dependent kinase; DAPI, 4′-6-diamidino-2-phenylindole; EMSA, electrophoretic mobility shift assay; GST, glutathione-*S*-transferase; PBS, phosphate-buffered saline; STAT, signal transducer and activator of transcription.

10.1021/bi052490j CCC: $33.50
Published on Web 04/12/2006

Nocodazole, vinblastine, colchicine, and paclitaxel are a group of structurally diverse microtubule-interfering agents, some of which have now been routinely used in tumor chemotherapy by virtue of their cell cycle arresting and apoptosis-inducing properties (*20*). Analyses of the cellular responses to microtubule disruption induced by nocodazole using Kinetworks multi-immunoblotting screens that utilize large panels of phospho-site antibodies have revealed numerous interesting changes in phosphorylation state of cell signaling proteins, some of which have been reported previously (*21, 22*).

In the present study, we set out to investigate another nocodazole-induced phosphorylation event, i.e., at STAT3 S727. We show that cyclin-dependent kinase 1 (CDK1) is the direct upstream protein kinase responsible for STAT3 S727 phosphorylation elicited by nocodazole treatment. Blocking S727 phosphorylation by replacing the serine residue with an alanine (S727A) resulted in elevated STAT3 DNA-binding activity, pointing to an inhibitory effect of S727 phosphorylation on STAT3 transcriptional activity. Examining cell cycle progression of the cells expressing STAT3 S727A indicated that phosphorylation of STAT3 S727 contributes to the mitotic arrest induced by nocodazole, and may play a role in regulating the onset and progression of M-phase during the cell cycle.

EXPERIMENTAL PROCEDURES

Antibodies and Chemicals. Rabbit polyclonal antibodies that recognize phospho-STAT3 S727, phospho-JAK1 Y1022/1023, JAK1, CDK1, and phospho-CDK1 T14/Y15 were purchased from BioSource (Camarillo, CA). Antibodies against STAT3, phospho-STAT3 Y705, and phospho-4E-BP1 T70 were from Cell Signaling Technology (Beverly, MA). Anti-p21$^{Waf1/Cip1}$, p27^{Kip1} , CDC25C, actin antibodies, and HRP-conjugated secondary antibodies were from Santa Cruz Biotechnology (Santa Cruz, CA). Anti-Flag rabbit polyclonal antibodies, anti-5′-bromo-2′-deoxyuridine (BrdU) mouse monoclonal antibodies, and BrdU were from Sigma (South San Francisco, CA). Active CDK1/Cyclin B1 and CDK2/Cyclin A were from Upstate Biotechnology Incorporation (UBI, Lake Placid, NY). Alexa488-labeled anti-mouse IgG and Alexa568-labeled anti-rabbit IgG were from Molecular Probes (Eugene, OR). Various protein kinase inhibitors were bought from Calbiochem (San Diego, CA). All other chemicals including microtubule-interfering agents were purchased from Sigma, unless otherwise stated.

Cell Lines and Culture Conditions. HeLa (human cervical carcinoma) and HEK293 (human embryonic kidney) cells were maintained in Dulbecco's modified Eagle medium (DMEM, GIBCO-BRL, Burlington, ON, Canada) supplemented with 10% fetal bovine serum (FBS, GIBCO-BRL), penicillin (100 units/mL) and streptomycin (100 μg/mL), in a humidified atmosphere containing 5% CO_2. The culture dishes used for HEK293 cells were treated with 10 μg/mL poly-L-lysine for 20 min prior to each use.

Plasmids. The pGEX plasmids containing glutathione-*S*-transferase (GST)-STAT3 wild-type (WT) and STAT3 point mutations at S727 (replaced by A, S727A) or Y705 (replaced by F, Y705F) were constructed as described previously (*23*). The STAT3 expression plasmids for mammalian cell transfection experiments were prepared in pXJ40-FLAG vector (*15*). The Flag sequences were incorporated into their C-termini as tags.

Transient Transfection. At 40−60% confluency, HEK293 cells were transiently transfected with plasmids as indicated using Lipofectamine transfection reagent (GIBCO-BRL) according to the manufacturer's protocol. Transfection medium was removed and cells were incubated in complete DMEM for 48 h to allow STAT3 expression prior to nocodazole treatment for 20 h. Transfection efficiency with various STAT3 expression vectors was estimated to be around 70%.

Phosphotransferase Activity Assay. For CDK activity assay in vitro, 5 μg of active CDK1/cyclin B1 was incubated with 5 μg of GST fusion proteins in 50 μL of CDK1 assay buffer (25 mM β-glycerol phosphate, 20 mM MOPS, 5 mM EGTA, 2 mM EDTA, 20 mM $MgCl_2$, 0.25 mM dithiothreitol, 5 μM β-methyl aspartic acid, and 100 μM ATP, pH 7.2) at 30 °C with the addition of 1 μCi/μL [γ-^{32}P]ATP. The reaction was stopped by the addition of SDS−PAGE sample buffer.

STAT3 DNA-Binding Activity Assays. For electrophoretic mobility shift assays (EMSA), 20 μg of total HEK293 cell lysates was used in each assay. Assays were carried out using STAT3 gel shift oligonucleotide from Santa Cruz Biotechnology prelabeled with [γ^{32}P]ATP (Amersham, Piscataway, NJ), according to the manufacturer's instructions. The resulting protein/DNA complexes were immunoprecipitated using anti-Flag antibody, and then resolved on a 13% native polyacrylamide gel. Signals were detected using a fluorescence imaging analyzer (BAS-5000) (Fuji film). A nonradioactive STAT3 transcription factor assay utilizing two STAT3 consensus binding sequences that are distinct from the one in EMSA was performed to confirm the results of EMSA, following the supplier's protocol (Chemicon, Temecula, CA).

Kinetworks Proteomics Analysis. Total cell lysates were prepared as described previously (*21*). Briefly, cells were washed with ice-cold PBS, scrapped in lysis buffer [pH 7.4, 20 mM Tris, 20 mM β-glycerophosphate, 150 mM NaCl, 3 mM EDTA, 3 mM EGTA, 1 mM Na_3VO_4, 0.5% Nonidet P-40, and 1 mM dithiothreitol] supplemented with protease inhibitors [1 mM phenylmethanesulfonyl fluoride (PMSF), 2 μg/mL leupeptin, 4 μg/mL aprotinin, and 1 μg/mL pepstatin A], and sonicated for 15 s. Cell debris was removed by centrifugation at 100 000 rpm for 30 min at 4 °C. For Kinetworks KPSS-1.1 phospho-site analysis, 300 μg of total protein was resolved on a 13% single-lane SDS polyacrylamide gel, transferred to nitrocellulose membrane. Using a 20-lane multiblotter from Bio-Rad (Hercules, CA), the membrane was incubated with different mixtures of up to 3 antibodies per lane that react with a distinct subset of at least 36 known phosphorylation sites in cell signaling proteins of distinct molecular masses. After further incubation with a mixture of relevant HRP conjugated secondary antibodies (Santa Cruz Biotechnology), the blots were developed using ECL Plus reagent (Amersham) and signals were quantified using Quantity One software (Bio-Rad). The panel of target phosphoproteins tracked in the Kinetworks KPSS-1.1 screen are listed in Figure 1. The Kinetworks KCCS 1.0 cell cycle protein analysis includes 30 pan-specific antibodies against major cell cycle related proteins, some of which are shown in Figure 10. Sample preparation and blot probing were performed similarly as those for KPSS-1.1. Detailed infor-

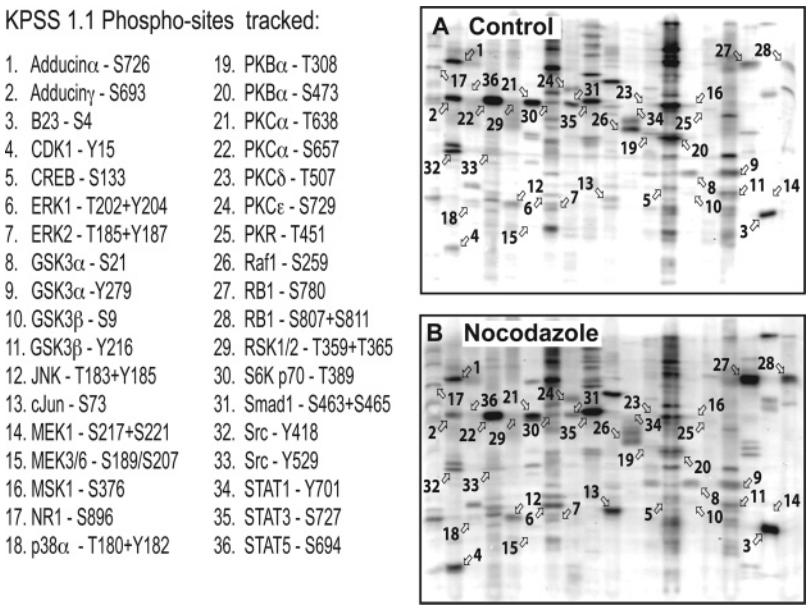

FIGURE 1: Kinetworks KPSS-1.1 phospho-site profile of HeLa cells in response to 200 ng/mL nocodazole treatment for 20 h. The phosphoprotein targets of 36 phospho-specific antibodies applied in the analysis are listed in the left columns. The expected migration positions of each of the target phosphoproteins are indicated with numbered arrows corresponding to the phospho sites indicated in the list. Changes in the intensity of many phosphorylation signals are evident in nocodazole-treated cells (B) as compared to DMSO-only-treated control cells (A). The STAT3 S727 phosphorylation signal, indicated as band 35, displayed one of the most striking increases in phosphorylation following nocodazole treatment.

mation and protocols of the Kinetworks analyses have been published previously (*24*) and can also be found at the Kinexus Bioinformatics Corp. Web site (www.kinexus.ca).

Flow Cytometry. Twenty-four hours after being transfected with STAT3 WT or S727A, HEK293 cell cultures were replated into new dishes to prevent overconfluence. Nocodazole treatment was administered at 24 h after replating for 20 h. Following trypsinization, cells were fixed in cold methanol and stained with propidium iodide in the presence of RNase A. The DNA fluorescence was measured using a FACScan (BD Biosciences, San Jose, CA); data acquisition and analysis were performed with the CellQuest software (Becton Dickinson).

BrdU Incorporation Assays and Immunofluorescence Microscopy. STAT3 WT, S727A-transfected HeLa cells grown on coverslips were treated with nocodazole for 20 h. After nocodazole was removed by rinsing the cells with PBS, and cells were then continuously incubated in the fresh medium containing 20 μM BrdU for 6 h. Cells were then fixed in 4% paraformaldehyde in PBS for 15 min at room temperature. After being permeabilized in methanol for 5 min, cells were resuspended in 2 M hydrochloric acid for 30 min followed by staining with anti-BrdU and anti-Flag antibodies for 2 h at room temperature. Their respective signals were detected by Alexa488-labeled anti-mouse IgG and Alexa569-labeled anti-rabbit IgG secondary antibodies for 1 h in the dark. Nuclei were counterstained with DAPI following RNaseA digestion. Cells were observed and images were collected under a Nikon fluorescence microscope, and images were analyzed using Northern Eclipse image software (Enpix, ON, Canada).

RESULTS

STAT3 S727 Phosphorylation Is a Mitosis-Associated Event. Exposure of proliferating HeLa cells to 200 ng/mL nocodazole for 20 h induced a cell-cycle arrest in mitosis sustained by the activation of the mitotic checkpoint control, accompanied by changes of a wide range of cell signaling proteins in phosphorylation states, as revealed by a Kinetworks phosphoprotein screen (KPSS-1.1) (*24*). This screen utilizes phospho-site-specific antibodies to systematically track changes in phosphorylation states of 30 known signaling proteins. As shown in Figure 1, numerous proteins involved in cell cycle regulation or stress/apoptosis responses exhibit either increased phosphorylation (e.g. B23 (nucleophosmin) S4, ERK1 T202+Y204, JNK T183+Y185, c-Jun S73 RB1 S780) or decreased phosphorylation (e.g. PKBα S473) upon nocodazole treatment as anticipated (*21*, *22*). Unexpectedly, phosphorylation of S727 in STAT3 was also enhanced by about 3.5-fold at 20 h upon nocodazole treatment. The phosphorylation increased gradually during the course of nocodazole treatment, reaching its maximum at around 20 h (Figure 2A,B). Treatment of HeLa with other microtubule-interfering agents such as paclitaxel, vinblastine, and colchicine at concentrations effective in causing the mitotic arrest also led to the increase of STAT3 S727 phosphorylation to different degrees (Figure 2C). No significant changes in STAT3 expression were observed upon treatment, indicating that the increase of S727 phosphorylation was not a result of the changes in STAT3 protein level (Figure 2D).

To determine whether the increase of STAT3 S727 phosphorylation was caused by the stresses elicited by microtubule interference or was a normal cell cycle event associated with mitosis, we monitored the level of STAT3 S727 phosphorylation in synchronized HeLa cells by releasing serum-starved cells from the G_0/G_1 block with serum addition. Whereas the STAT3 protein level remained relatively constant during the cell cycle, a maximum level of STAT3 S727 phosphorylation was detected at ~24 h post

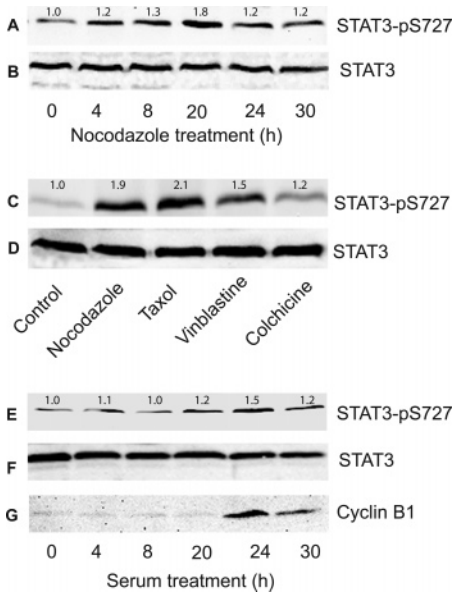

FIGURE 2: Phosphorylation of STAT3 S727 is associated with mitosis. Treatment of proliferating HeLa cells with 200 ng/mL nocodazole led to a gradual increase of STAT3 S727 phosphorylation, reaching the maximum at ~20 h upon the treatment (A, B). Images from one of three replicate experiments are presented here with quantification data of bands indicated in the figure. The average fold-change of S727 phosphorylation from 3 replicates was 1.93 ± 0.23 (mean ± SD). Treatment with various microtubule-interfering agents including nocodazole (200 ng/mL), paclitaxel (7 μM), vinblastine (1 μM), and colchicine (1 μM) at the concentrations effective in arresting the cell cycle in mitosis for 20 h enhances phosphorylation of STAT3 S727 (C) without affecting total STAT3 protein expression (D). Twenty-four hours after serum deprivation, serum was added back to medium to induce cells to re-enter the cell cycle synchronously. At time points indicated, cells were harvested and total lysates were prepared. The S727 phosphorylated STAT3 and the total STAT3 protein level were detected by immunoblotting with anti-phospho-STAT3 S727 and anti-STAT3, respectively (E, F), and the progression of the cell cycle was monitored by immunoblotting with anti-cyclin B1 (G). Images from one of three replicate experiments are presented here with quantification data of bands indicated in the figure. The average fold-change of S727 phosphorylation from 3 replicates was 1.53 ± 0.15 (mean ± SD).

serum addition (Figure 2E,F), coinciding with the time when the expression of cyclin B1 reached its peak (Figure 2G). The observation of the higher level of S727 phosphorylation in mitotic cells in the absence of microtubule disruption indicates that the increase of STAT3 S727 phosphorylation is a normal M-phase-associated event.

Reciprocal Inhibition between S727 and Y705 Phosphorylation. Concomitant to the increase of STAT3 S727 phosphorylation with treatment of HeLa cells with nocodazole for 20 h, there was a reduction of STAT3 phosphorylation at Y705 (Figure 3). Y705 phosphorylation is known to be critical for STAT3 dimerization and nuclear translocation upon its activation. The increase of S727 phosphorylation coincident with the reduction of Y705 phosphorylation in STAT3 upon nocodazole treatment indicated possible reciprocal regulation between these two phosphorylation events.

To further investigate this possibility, we examined the two phosphorylation events in HEK293 cells expressing wild-type (WT) STAT3 or nonphosphorylatable mutants, S727A or Y705F. Upon 20 h of nocodazole treatment, whereas the

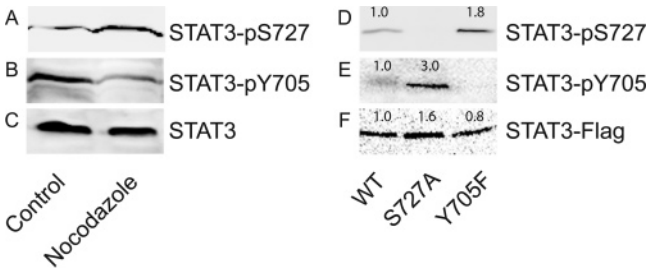

FIGURE 3: Reciprocal inhibition between S727 and Y705 phosphorylation in STAT3. Induction of STAT3 S727 phosphorylation (A) by nocodazole treatment (200 ng/mL for 20 h) of HEK293 cells was accompanied by repression of Y705 phosphorylation (B), without changes in total STAT3 protein levels (C) as detected with specific antibodies in the immunoblots shown (~90% increase in S727 versus 65% reduction in Y705 after they were normalized to the STAT3 total protein level). Transfecting HEK293 cells with STAT3 Y705F resulted in an elevated level of S727 phosphorylation immunodetection (D) in response to nocodazole treatment as compared to the cells transfected with STAT3 WT. Conversely, the cells transfected with STAT S727A exhibited an increase in Y705 phosphorylation immunodetection (E). The total levels of expression of wild-type and phosphorylation site mutants of STAT3 were examined by immunoblotting (F). Each protein detected in STAT mutant-transfected cells was quantified and normalized to its counterpart in STAT3 WT-transfected cells, and the numbers derived were indicated above the corresponding bands.

overexpression of STAT3 S727A mutant abrogated S727 phosphorylation as expected, a higher level of S727 phosphorylation was observed in STAT3 Y705F-expressing cells as compared to STAT3 WT-transfected cells (Figure 3D). Conversely, Y705 phosphorylation was further enhanced in S727A-expressing cells relative to that in WT-transfected cells. The expression levels of exogenous STAT3 WT, S727A, and Y705F were found to be comparable, as can be seen in Figure 3F. Not only did these findings reveal that the two phosphorylation events are regulated independently, but also they confirmed the suppressing effects of serine and tyrosine phosphorylation on each other.

CDK1 Phosphorylates STAT3 at S727. A number of protein kinases involved in various signaling pathways have been demonstrated to target either directly or indirectly STAT3 S727 phosphorylation with distinct consequences (*19*). To elucidate the pathway(s) that mediate STAT3 S727 phosphorylation induced by microtubule interference, several protein-serine/threonine kinase inhibitors were employed along with nocodazole to examine their effects on this phosphorylation event; these included the Mek1/2 inhibitor PD98059, the p38 MAPK inhibitor SB203580, the JNK1/2 inhibitor SP600125, the CK2 inhibitor DRB (5,6-dichloro-1-β-D-ribofuranosylbenzimidazole), the phosphatidylinositol 3-kinase inhibitor LY294002, the CDK1/2 inhibitor olomoucine, the mTOR inhibitor rapamycin, and the PKC inhibitor RO318220. Among them, only olomoucine perturbed nocodazole-induced S727 phosphorylation significantly, while no effects were observed on STAT3 protein expression, indicating the possible involvement of CDK1/2 in the pathway leading to S727 phosphorylation (Figure 4A,B). A similar inhibitory effect on STAT3 S727 phosphorylation was also observed in Roscovitine, another potent and selective inhibitor of CDKs (Figure 4C,D). Recently, alsterpaullone, belonging to a family of benzazepinones, was identified to be a highly specific and potent inhibitor for CDKs (*25*). Incubation of HeLa cells with 1 μM alster-

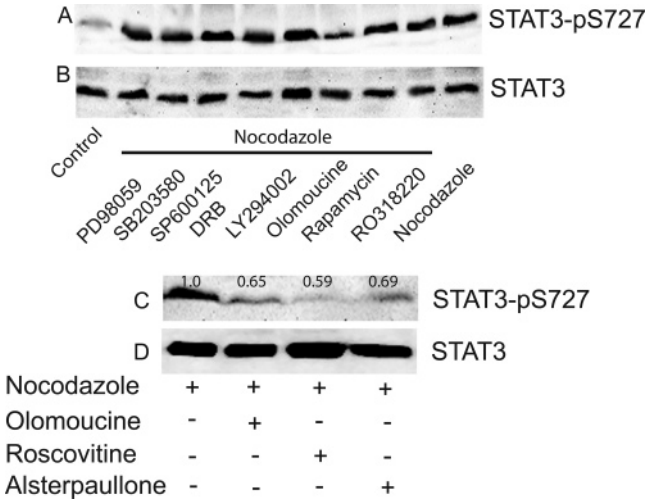

FIGURE 4: CDK1 is involved in STAT3 S727 phosphorylation. Protein kinase inhibitors including PD98059 (30 μM), SB203580 (5 μM), SP600125 (0.5 μM), DRB (20 μM), LY294002 (10 μM), olomoucine (50 μM), rapamycin (40 nM), and RO318220 (1 μM) were applied at the concentrations as indicated along with 200 ng/mL nocodazole for 20 h. The levels of STAT3 phosphorylation and total protein were detected by immunoblotting with anti-phospho-STAT3 S727 and anti-STAT3, respectively (A, B). Like olomoucine, two other CDK inhibitors with higher specificity for CDKs, roscovitine (10 μM) and alsterpaullone (1 μM), exhibited negative effects on STAT3 S727 phosphorylation (C, D). Phosphorylation of STAT3 at S727 was quantified and normalized to STAT3 total protein level, and the numbers derived were indicated above the corresponding bands.

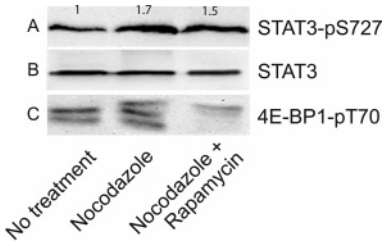

FIGURE 5: Rapamycin inhibits mTOR phosphotransferase activity but not STAT3 S727 phosphorylation. Rapamycin used in the experiment shown in Figure 4 inhibited the activity of its cognate target kinase mTOR, as indicated by the reduction of 4E-BP1 T70 phosphorylation (C). No effect on STAT3 expression (B) nor its S727 phosphorylation (A) was seen.

paullone, at a concentration for which only the activities of CDK1 (IC_{50} 0.035 μM), CDK2 (0.015 μM), and CDK5 (0.040) are known to be suppressed (*26*), led to a reduction of STAT3 S727 phosphorylation in nocodazole-treated cells (Figure 4C,D). Since CDK1 is the only CDK that exhibits significant activity during nocodazole-induced mitotic arrest, the suppressing effect of these three CDK inhibitors on STAT3 S727 phosphorylation is most likely to be attributed to their inhibitory effects on CDK1 activity.

All the inhibitors used in this study were applied in the concentrations effective in inhibiting the phosphotransferase activities of target protein kinases. For instance, whereas both STAT3 S727 phosphorylation and STAT3 protein level remained unaffected, the inhibition of mTOR kinase activity by rapamycin was clearly demonstrated by the fact that the nocodazole-induced phosphorylation 4E-BP1 T70, a target site of mTOR, was abrogated in the presence of rapamycin (Figure 5).

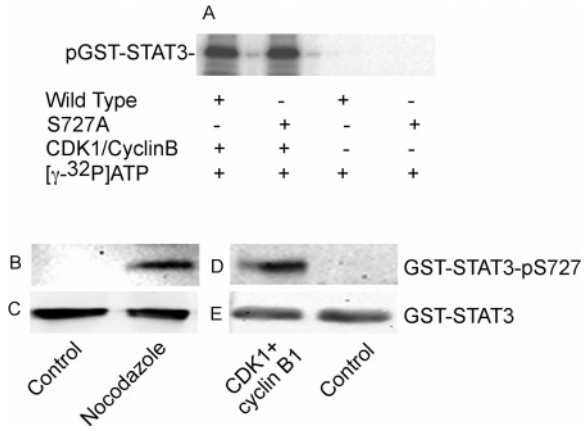

FIGURE 6: CDK1 is a direct STAT3 S727 kinase. Equal amounts of bacterially expressed GST-STAT3 WT and S727A fusion proteins were incubated with active CDK1/cyclin B1 complex expressed and purified from insect cells in an in vitro phosphorylation assay with [γ-^{32}P]ATP, and phosphorylation of STAT3 proteins was detected by autoradiography after proteins were resolved on SDS−PAGE (A). GST-STAT3 WT protein was incubated with total lysates of HeLa cells treated with either 200 ng/mL nocodazole or DMSO (control) for 20 h in CDK1 activity assay reactions. The increase of S727 phosphorylation on GST-STAT3 (B) was immunodetected after incubating with lysates from nocodazole-treated cells. Similarly, active CDK1/cyclin B1 complex exhibited strong STAT3 S727 phosphotransferase activity in vitro (D). The total level of GST-STAT3 by immunodetection is also shown in these experiments (C, E).

To confirm the role of CDK1 in STAT3 S727 phosphorylation, we tested whether STAT3 could be phosphorylated at S727 by CDK1 in vitro. Bacterially expressed GST-STAT3 WT fusion protein was found to be phosphorylatable by a purified active recombinant CDK1/cyclin B1 complex from transfected insect cells in vitro (Figure 6A). Surprisingly, disruption of the S727 phosphorylation site by substituting the serine with an alanine did not significantly affect the incorporation of [γ-^{32}P] into the fusion protein, implying possible existence of multiple CDK1 phosphorylation sites on STAT3 in vitro. Examination of human STAT3 protein sequence revealed at least another potential CDK1 phosphorylation at T714 in addition to S727 (data not shown). To further address this question, the phospho-STAT3 S727 antibody was used in immunoblot analysis to probe the GST-STAT3 WT fusion protein preincubated with the lysate from nocodazole-treated HeLa cells, which is expected to contain a higher level of CDK1 activity than that from control nontreated cells. As shown in Figure 6B,C, incubation with nocodazole-treated lysate resulted in an increase in STAT3 phosphorylation at S727. Similar to the lysate preparation from nocodazole-treated HeLa cells, active CDK1/cyclin B1 phosphorylated GST-STAT3 at S727, indicating that CDK1 is capable of phosphorylating STAT3 S727 directly in vitro (Figure 6D,E).

To further explore the possible regulation of STAT3 S727 phosphorylation by CDK1, we next investigated whether CDK1 directly interacted with STAT3 in vivo. Reciprocal immunoprecipitations with either CDK1 or Flag antibody were carried out in lysates of HEK293 cells transfected with either a Flag-tagged STAT3 WT or a S727A mutant construct, followed by nocodazole treatment for 20 h. Interestingly, the interaction between two proteins was little to none in cells that overexpressed STAT3 WT protein which was expected to be highly phosphorylated at S727 upon

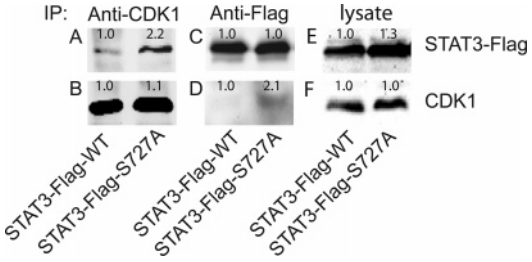

FIGURE 7: CDK1 and STAT3 form complexes in vivo. CDK1 or STAT3 proteins were immunopreciptated from the lysates of HEK293 cells transfected with either Flag-tagged STAT3 WT or S727A constructs followed by nocodazole treatment (200 ng/mL for 20 h) with anti-CDK1 or anti-Flag antibodies. The levels of target proteins were detected by immunoblotting with the same antibodies (B, C). A higher level of STAT3 S727A was present in anti-CDK1 immunoprecipitates than STAT3 WT (A). CDK1 was detected in complex with STAT3 S727A whereas CDK1 was almost undetectable in STAT3 WT immunoprecipitates (D). The levels of exogenously expressed Flag-STAT3s and endogenous CDK1 were examined by immunoblotting with their respective antibodies (E, F). Each protein detected in STAT3 S727A-transfected cells was quantified and normalized to its counterpart in STAT3 WT-transfected cells, and the numbers derived were indicated above the corresponding bands.

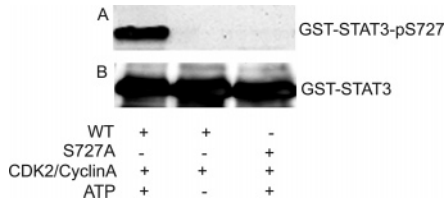

FIGURE 8: CDK2 can phosphorylate STAT3 at S727 in vitro. GST-STAT3 WT protein was phosphorylated by active CDK2/Cyclin A in vitro at S727, as detected by anti-phospho-STAT3 S727 antibody, which was abrogated by mutation of S727 to A727 (A,B).

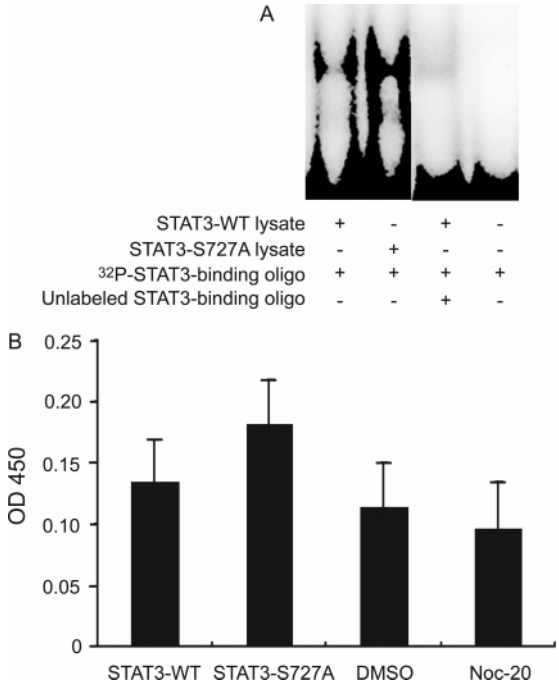

FIGURE 9: Inhibition of S727 phosphorylation enhances STAT3 DNA-binding activity. The DNA-binding activities of STAT3 WT and S727A were analyzed by an electrophoretic mobility shift assay (A) or a nonradioactive transcription assay using 2 other STAT3 consensus binding sequences (B). In EMSA, a ^{32}P-labeled STAT3 consensus binding oligonucleotide was used and the binding of STAT3 was revealed by autoradiography. The binding activity was blocked by the presence of the unlabeled STAT3 binding oligonucleotide and the absence of cell lysate. In nonradioactive assay, the binding of STAT3 to its target oligonucleotides was detected by a STAT3 antibody in an ELISA format at 450 nm wavelength.

nocodazole treatment (Figure 7). In contrast, a stronger interaction was found between CDK1 and STAT3 S727A. The differential affinity of CDK1 for STAT3 WT and STAT3 S727A appears to be consistent with the kinetic relationship between an enzyme and a pseudosubstrate. Together, the results further strengthen the notion that CDK1 is a direct upstream protein-serine kinase of STAT3.

Given the broad-specificity nature of the CDK inhibitors used above, we were interested to find out if STAT3 S727 phosphorylation was specific for CDK1. An active CDK2/cyclin A complex was incubated with purified GST-STAT3 WT protein in vitro, and the phosphorylation state of S727 was monitored by immunoblotting with anti-phospho-STAT3 S727 antibody. As shown in Figure 8, active CDK2/cyclin A phosphorylated STAT3 WT at S727, which was completely abrogated in the assay where STAT3 S727A mutant was used instead. The result indicated that both CDK1 and CDK2 are capable of phosphorylating STAT S727 in vitro.

STAT3 S727 Phosphorylation by CDK1 Attenuates Its DNA-Binding Activity. Despite accumulating evidence for the importance of STAT3 serine phosphorylation, its effect on the STAT3 DNA-binding/transcriptional activity remains controversial. To elucidate the effect of CDK1-mediated S727 phosphorylation, we compared the DNA-binding activities of STAT3 WT and STAT3 S727A overexpressed in HEK293 toward a double-stranded oligonucleotide containing the consensus binding site for STAT3 (5′-GAT CCT TCT GGG AAT TCC TAG ATC-3′) in electrophoretic mobility shift assays (EMSAs). As shown in Figure 9A, while both proteins were expressed at similar levels, more STAT3 S727A proteins were found in complexes with DNA in the STAT3 immunoprecipitates than STAT3 WT, indicating that STAT3 S727A possesses stronger DNA-binding activity when compared to its wild-type counterpart. The specificity of STAT3 DNA-binding activity to its target sequence was evident as the binding was disrupted by the inclusion of unlabeled same target sequence in the assays. No binding signal was detected in the absence of cell lysate. Similarly, the enhanced DNA-binding affinity of STAT3 S727A was also observed when two other STAT3 binding oligonucleotide sequences were used in a nonradioactive transcription assay (Figure 9B).

The stronger DNA-binding activity of STAT3 S727A as compared to STAT3 WT implies that phosphorylation of S727 in STAT3 inhibits its interaction with its target genes and presumably its transcriptional activity. However, as demonstrated earlier, phosphorylation of STAT3 at Y705 was upregulated when S727 phosphorylation was suppressed, which might be attributed to the increase of the DNA-binding activity of STAT S727A mutant. To exclude the interference that might come from Y705 phosphorylation, we used bacterially expressed STAT3 S727A and STAT3 WT proteins preincubated with active CDK1/cyclin B1 complex for 0.5 h at 30 °C in a nonradioactive transcription assay as described above. Without Y705 phosphorylation, STAT3 S727A protein exhibited approximately 20% higher DNA-binding activity toward putative STAT3 recognition motif

than its wild-type counterpart ($p < 0.01$), indicating that the S727 phosphorylation plays a direct role in regulating the DNA-binding activity of STAT3, regardless of the phosphorylation state of Y705 (data not shown).

Inhibition of S727 Phosphorylation Abolishes Nocodazole-Induced Mitotic Arrest. Since STAT3 S727 phosphorylation is a cell cycle related event, we set out to investigate the physiological role of its phosphorylation by examining the effect of STAT3 S727A mutant expression on cell cycle progression. The cell cycle analysis of the STAT3 S727A-transfected cells using flow cytometry revealed no effects on cell cycle progression upon the disruption of STAT3 S727 phosphorylation (data not shown). As expected, about 50% of the cell population transfected with STAT3 WT accumulated in a tetraploid (4*N*) state upon a 20 h nocodazole treatment (Figure 10A,B). Examination of cell morphology as well as chromosome configuration indicated that most cells were in mitotic arrest induced by nocodazole. In sharp contrast, transfection with STAT3 S727A resulted in the accumulation of around 70% of the cells in 2*N* DNA states while only less than 5% of the cells remained as 4*N*, indicative of a cell cycle arrest at the G1 phase (Figure 10C,D). No significant difference in the percentage of cells with DNA content more than 4*N* was observed between STAT3 S727A- and WT-transfected populations, indicating that blocking S727 phosphorylation did not result in defects in nuclear division/cytokinesis in the cells that had passed the G1/S transition. One possible explanation for the decrease of 4*N* cells coupled with the increase of 2*N* cells was a loss of the mitotic arrest induced by nocodazole and exit of the cells into the next G1 phase where they remained. Another possibility was that the cells expressing STAT3 S727A have a prolonged G1 phase upon nocodazole treatment.

To examine the underlying mechanisms, we evaluated the effects of STAT3 S727A transfection on the expression of 30 cell cycle related proteins including various CDKs, cyclins, CDK inhibitors, and other key proteins involved in the control of the entry in, progression through, and withdrawal from the cell cycle using the Kinetworks KCCP-1.0 cell cycle protein analysis (Figure 11A). In particular, in the STAT3 S727A transfected HEK293 cells, the expression levels of CDK4, CDK5, NEK2, 14-3-3, and $p27^{Kip1}$ CDK inhibitor were elevated greater than 1.6-fold, and the expression levels of Cdc34, CDK7, and cyclin G1 were reduced by more than 50% (Figure 11B). The expressions of an additional 8 known STAT3 target genes such as Mcl-1, Bcl-2, c-Myc, and c-Fos were also examined in STAT3 WT and S727A-transfected HEK293 cells following a 20 h nocodazole treatment (data not shown). Whereas most of the cell cycle proteins as well as STAT3 targets remained essentially unaltered in their protein levels upon inhibition of S727 phosphorylation, the expression of two CDK inhibitors, $p21^{CIP1/WAF1}$ (Figure 12A, H) and $p27^{Kip1}$(Figure 12B,I), in STAT3 S727A-transfected cells was at least 80% and 37%, respectively, higher than that of WT-transfected cells at 20 h following the addition of nocodazole. Moreover, whereas cyclin E, a cyclin that is known to be in complex with and activate CDK2 and involved in the G1/S transition, was barely detectable in WT-transfected cells arrested at the M phase as expected, transfection of S727A led to a 118% increase in cyclin E expression (Figure 12C,J). (Greater amounts of total cell lysates as well as higher concentrations

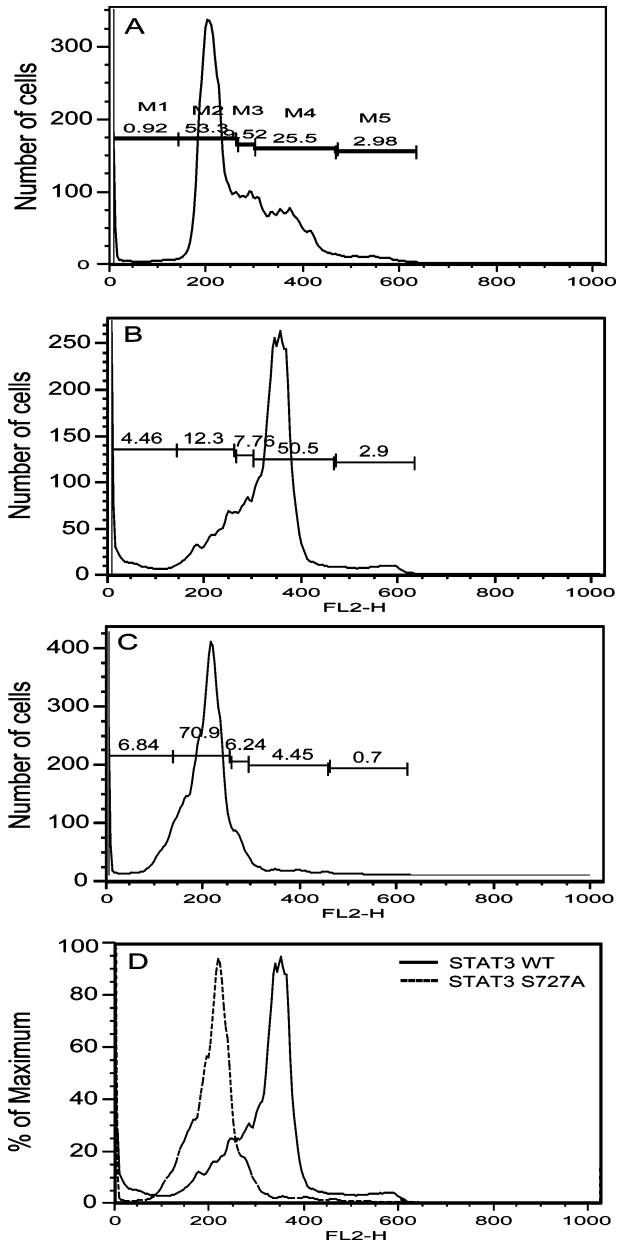

FIGURE 10: Inhibition of S727 phosphorylation results in the loss of mitotic arrest induced by nocodazole and a G1 arrest in the next cell cycle. HEK293 cells were transfected with STAT3 WT (A, B) or STAT3 S727A (C) followed by DMSO (A) or nocodazole treatment (B, C) for 20 h. The cell cycle profile was assessed by flow cytometry based on DNA content. DNA content is represented on the *X*-axis (FL2-H); the number of cells counted is represented on the *Y*-axis in A, B, and C. The percentage of cells with defined DNA content is indicated in the figure: M1, $<2N$ (sub-G1); M2, $2N$ (G1); M3, $2N-4N$ (S); M4, $4N$ (G2/M); M5, $>4N$. Panels B and C are overlaid on each other in D to exemplify the difference in the cell cycle profile.

of anti-p21 and anti-cyclin E antibodies were used in the experiment shown in Figure 12 than in the KCCP 1.0 cell cycle protein screen to permit better detection of their target proteins.) In contrast, the expression of CDC25C, a dual specificity phosphatase responsible for removing phosphate groups from the inhibitory T14 and Y15 phosphorylation sites of CDK1 at the G2/M transition, so as to activate its kinase activity, was decreased 25% when S727 phosphorylation was suppressed (Figure 12D,K), which would contribute to the 525% increase of T14/Y15 phosphorylation

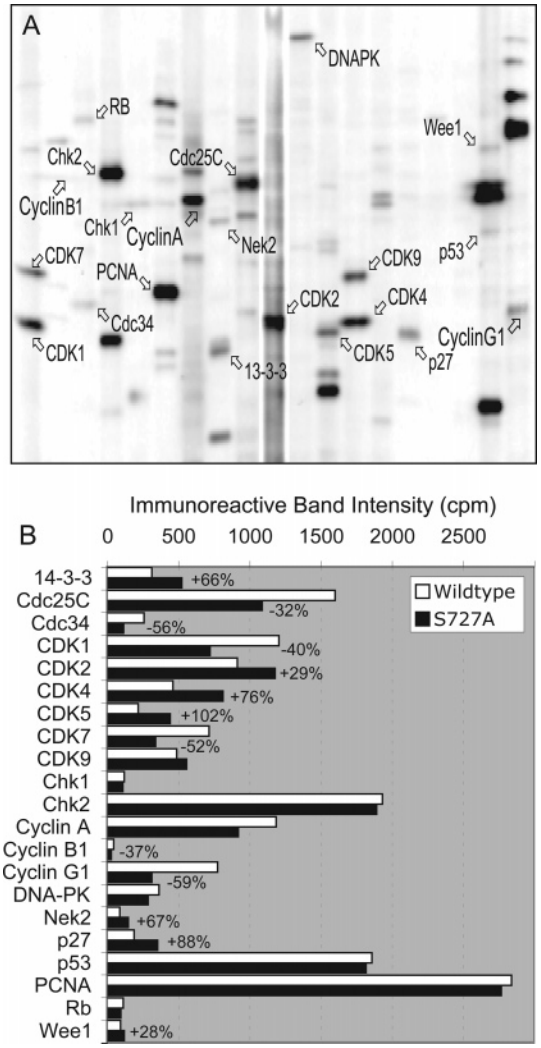

FIGURE 11: Effects of STAT3 S727 phosphorylation on the expression of cell cycle regulatory proteins. The expressions of 30 cell cycle proteins were examined in HEK293 cells transfected with STAT3 WT or S727A followed by nocodazole treatment (200 ng/mL for 20 h) using the Kinetworks KCCP-1.0 cell cycle protein analysis. Only 21 of the target proteins were detected in these cells, and their mobility positions are indicated in panel A, which is a representative immunoblot from STAT3 S727A mutant transfected cells. The quantification of the intensity of the immunoreactive target protein bands detected by ECL for STAT3 WT (white bars) and S727A mutant (black bars) transfected cells is shown in panel B, along with percent changes in band intensity greater than 25%. The reproducibility of Kinetworks analyses on the same sample in different immunoblots is typically within 85%.

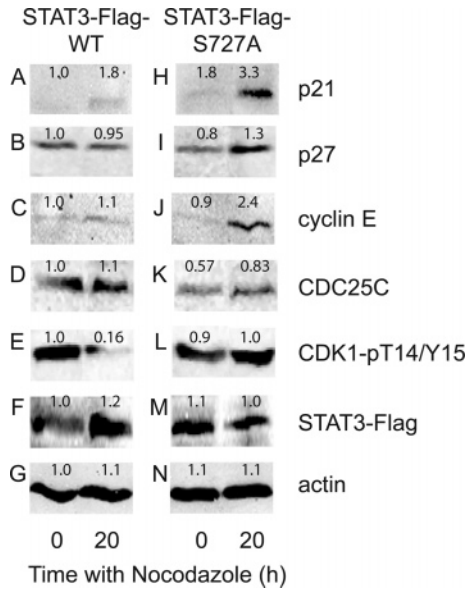

FIGURE 12: Expression of cell cycle regulatory proteins in STAT3 S727A is consistent with a G1 arrest in the cell cycle. The protein levels of $p21^{CIP1/WAF1}$ (A, H), $p27^{Kip1}$ (B, I), cyclin E (C, J), CDC25C (D, K), and phosphorylation of CDK1 T14/Y15 (E, L) were examined in HEK293 cells transfected with STAT3 WT (A−G) or S727A (H−N) at 20 h after 200 ng/mL nocodazole addition by immunoblotting with their respective antibodies. Transfected cells treated with DMSO were used as controls. Expression of STAT3 constructs was monitored using a STAT3 antibody (F, M), and actin was used as the loading control (G, N). Each protein detected was quantified and normalized to the level of the protein in STAT3 WT-transfected cells at time 0 h without nocodazole treatment, and the numbers derived were indicated above the corresponding bands.

on CDK1 in S727A-transfected cells (Figure 12L). The profiles of CDK1 T14/Y15 phosphorylation state and the protein levels of CDC25C and cyclin E as well as the morphology of nuclei of cells at several time points over the course of nocodazole treatment indicated that the STAT3 S727A cells progressed through the M phase as STAT3 WT cells did after the addition of nocodazole, but failed to arrest at the M phase. Instead, they slipped into the next cell cycle and arrested at G1.

Taken together, the expression-related changes of the above cell cycle proteins seem to point to the abrogation of nocodazole-induced mitotic arrest upon the inhibition of S727 phosphorylation, which is in agreement with the observations derived from flow cytometry analysis.

If the STAT3 S727A-expressing cells were arrested in the G1 phase as indicated above, it is anticipated that they will enter the S phase (DNA synthesis) sooner than their wild-type counterparts when they are released from nocodazole treatment. To this end, we monitored the incorporation of BrdU, a thymidine analogue, into nuclear DNA for 6 h after nocodazole was removed (Figure 13). Over 60% of STAT3 S727A cells exhibited the BrdU incorporation at 6 h after nocodazole removal (Figure 13C,D). In contrast, less than 15% of STAT3 WT cells were BrdU-positive (Figure 13A,B). The results further strengthen the notion that STAT3 S727 phosphorylation plays a critical role in nocodazole-induced mitotic arrest.

DISCUSSION

The onset of mitosis is accompanied by a series of reversible phosphorylation/dephosphorylation events that modulate profound changes in cellular architecture including nuclear envelope breakdown, nuclear lamina depolymerization, chromosome condensation, and microtubule reorganization. Systematic examination of mitosis-associated phosphorylation events using Kinetworks phosphoprotein analyses by tracking the precise phosphorylation states of a large number of signal transduction proteins simultaneously has begun to offer in-depth views of the interconnective nature of the cell signaling pathways that orchestrate various cell cycle events (*22*).

In the present study, we focused our attention on one of the phosphorylation events initially identified in nocodazole-treated HeLa cells, i.e. STAT3 S727 phosphorylation. Despite

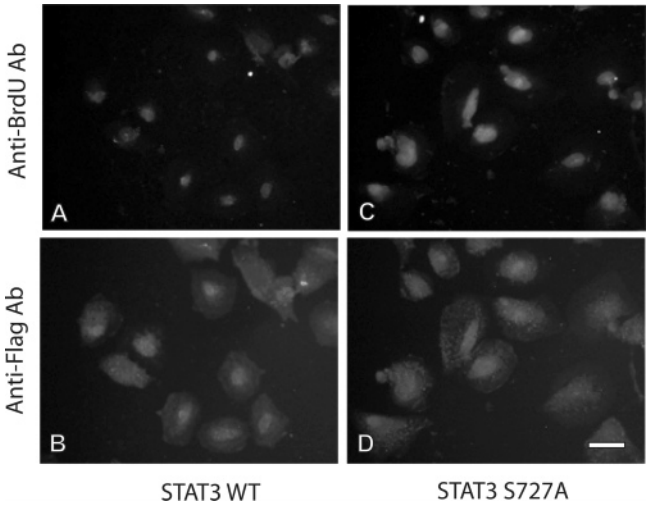

FIGURE 13: Upon the release from nocodazole treatment, the STAT3 S727A-expressing cells enter the S phase sooner than the cells expressing STAT3 WT. STAT3 S727A (C, D) and WT-transfected (A, B) HeLa cells were treated with nocodazole for 20 h. Nocodazole was then removed and the cells were incubated with BrdU for 6 h. Incorporation of BrdU into nuclei was monitored by anti-BrdU antibody (A, C), and the expression of STAT3 S727A and WT was detected with anti-Flag antibody (B, D). Bar, 10 μm.

the facts that the serine residue was first characterized about 10 years ago as a second phosphorylation site after tyrosine in most of STAT family members, and its important roles in modulating STATs' transcriptional activity has since been well recognized, the signaling pathways leading to its phosphorylation, its functional consequences, and the interrelationship between tyrosine and serine phosphorylation were unresolved (*19*). Numerous studies have demonstrated that various proline kinases including members of the MAPK family are implicated in the serine phosphorylation of STATs early in the G1 phase of the cell cycle following mitogenic stimuli. The characteristics of the flanking amino acid sequences surrounding the serine phosphorylation site where a proline residue is located at +1 position [i.e. P(M)SP] conform to MAPK phosphorylation site consensus sequences (*27*). Surprisingly, based on the effects of a panel of inhibitors specific for various protein-serine/threonine kinases, our data pointed to the involvement of another group of proline-directed kinases, i.e. cyclin-dependent kinases (CDKs) in mediating the serine phosphorylation of STAT3 in response to nocodazole treatment. The specificity of putative CDK inhibitors employed in this study is further supported by the fact that no significant effect of the inclusion of olomoucine in nocodazole treatment on the phosphorylation states of a wide range of cell signaling proteins in Kinetworks phosphoprotein profiling was observed. While active CDK2/cyclin A complex also exhibited STAT3 S727 phosphorylation activity in vitro, the relationship between CDK1 and STAT3 S727 phosphorylation is supported by the close temporal correlations between serine phosphorylation and CDK1 activation both at the onset of the M phase and in mitotic arrest induced by nocodazole. The direct enzyme/substrate relationship between CDK1 and STAT3 is further strengthened by the evidence of in vitro STAT3 S727 phosphorylation activity of CDK1/cyclin B1 complex and the in vivo interaction between CDK1 and mutant STAT3 with an unphosphorylatable residue substituted at the S727 site.

The gradual increase of STAT3 S727 phosphorylation during the time-course experiments with a moderate 2-fold change at 20 h after nocodazole treatment coinciding with the onset of the M phase might be attributed to the low synchrony of cell cycle in the cell population used as well as the possible involvement of other CDKs activated early during the cell cycle in STAT3 S727 phosphorylation, as exemplified by the CDK2 STAT3 S727 phosphorylation activity in vitro. This might at least in part account for the difficulty in seeing dramatic effects on the cell cycle progression upon the knockout of the S727 site in the absence of nocodazole treatment. The treatment with nocodazole leads to the ultimate synchronization of the cell cycle, which might amplify the phenotypic effects derived from the deficiency in the S727 phosphorylation mediated by CDK1.

In keeping with our finding of the involvement of CDK1 in modulating STAT3 serine phosphorylation, a previous study has shown that cyclin D/CDK4 and cyclin E/CDK2 were in complexes with STAT92E, a STAT3 homologue in *Drosophila*, and regulated STAT92E protein stability, which in turn mediated the roles of CDK4 and CDK2 in fly developmental processes (*28*). However, no direct STAT3 serine phosphorylation activity was ascribed to either CDK4 or CDK2. More recently, in a screen for potential substrates of CDK5, a cyclin-dependent kinase implicated in neuronal migration and synaptic plasticity, Fu et al. (*29*) demonstrated that STAT3 was phosphorylated by CDK5/p35 at S727 both in vitro and in vivo and the CDK5-mediated serine phosphorylation enhanced STAT3 transcriptional activity. But, unlike most CDK family members, CDK5 is not involved in the cell cycle regulation and only exhibits kinase activity in neurons where its activator p35 is exclusively expressed (*30*). Thus, to our knowledge, our study provides the first experimental evidence for a direct link between CDK1, the master regulator of eukaryotic cell cycle progression at the M phase, and a member of signal transducers and activators of transcription family (STATs).

Despite the well-established roles of tyrosine phosphorylation in dimerization and nuclear translocation, a prerequisite for STAT activation, it is now becoming more and more evident that the effects of phosphorylation on STAT's DNA-binding and/or transcriptional activities are far more complex than initially thought, at least in part due to the conflicting reports on the interrelationship between serine and tyrosine phosphorylation under different experimental settings. In our study, an inverse correlation between serine and tyrosine phosphorylation states was observed in response to nocodazole treatment, implying that neither serine nor tyrosine phosphorylation is a prerequisite for phosphorylation of the other and the phosphorylation of these two residues is regulated independently. The inhibitory effect of these two phosphorylation events was clearly demonstrated in non-phosphorylatable mutant S727A or Y705F-transfected cells in which higher levels of serine or tyrosine phosphorylation were observed when the phosphorylation of the other residue was repressed. The reciprocal suppression effects cannot be attributed to the changes in activities of their respective upstream kinases, as the activities of CDK1 and JAK1 remained unaltered in either of the mutant-expressing cells (unpublished data, Pelech et al.). However, it cannot be excluded that phosphorylation of either the serine or tyrosine residue may exert a positive impact on the dephosphorylation

of the other. In contrast to extensive studies focused on protein kinases that target STAT3, little is known regarding protein phosphatases responsible for STAT3 dephosphorylation. It is possible that the increase of STAT3 S727 phosphorylation associated with mitosis as observed in this study might result from the inhibition of protein phosphatase(s) targeting S727. Protein phosphatase 2A (PP2A) has been found to be involved in STAT3 S727 dephosphorylation in response to angiotensin II *(31)*.

While most evidence supports a positive role for S727 phosphorylation in STAT3 DNA-binding/transcriptional activation (*8*, *10*, *30*, *32*), it has also been documented that mutation of STAT3 S727 did not exhibit any effect on STAT3 DNA-binding activity (*11*, *12*). More recently, there is emerging evidence for a negative role for serine phosphorylation, although its underlying mechanism is unclear (*11*, *15*, *19*). The conflicting reports on the effects of S727 phosphorylation on STAT3 transcriptional activity may be at least partly due to the involvement of multiple signaling pathways in its phosphorylation in response to diverse activation signals. Our study revealed that STAT3 S727A displayed enhanced DNA-binding activity toward an oligonucleotide containing STAT3 binding site as compared to its WT counterpart, indicating that S727 phosphorylation exerts an inhibitory effect on STAT3 DNA-binding activity. This seems to be in agreement with the inhibitory effect of S727 phosphorylation on the phosphorylation of Y705, which was observed in this study and by others in previous reports. Therefore, our data demonstrates a negative effect of S727 phosphorylation implicated in modulating STAT3 DNA-binding activity, and presumably transcriptional activity, in nocodazole-induced mitotic arrest.

Contrary to the usual mitotic arrest observed for most cells upon nocodazole treatment, the defect in STAT3 S727 phosphorylation leads to the accumulation of cells with 2*N* DNA content accompanied by the reduction of 4*N* cells, indicative of an exit from mitotic arrest with successful completion of cytokinesis followed by an arrest in the following the G1 phase. The loss of mitotic arrest in S727A cells is supported by the reduced expression of CDC25C, a positive regulator of the onset of the M phase, whereas the resulting G1 arrest is consistent with the enhanced expression of various G1 cell cycle proteins such as $p21^{CIP1/WAF1}$, $p27^{Kip1}$, and cyclin E. As members of the Cip/Kip family of CDK inhibitors, the expression of both $p21^{CIP1/WAF1}$ and $p27^{Kip1}$ is controlled through the programmed protein degradation by ubiquitin-mediated proteolysis and/or the p53 family protein-dependent transcriptional regulation in response to the stresses as a result of DNA damages and apoptosis *(33)*. They have also been known to be STAT3 target genes as evidenced by the presence of STAT1 and STAT3 binding sites in their promoters (*34*−*36*). Both p53-dependent induction of p21 and p53-independent induction of p21 have been documented that are required for the cell cycle arrest at G1/S in response to activation of either the DNA damage checkpoint or the spindle assembly checkpoint (*37*, *38*). In our study, the increased expression of $p21^{CIP1/WAF1}$and $p27^{Kip1}$ did not seem to affect the onset of mitosis, as indicated by the lack of significant increase in the cell population with polyploidy. Therefore, we speculate that the potential inhibition of CDK1 activity during the M phase by the elevated levels of both CDK inhibitors may promote the cells to undergo an exit from mitosis.

Based on our observations in this study along with other reports, it is tempting to propose a hypothesis to address the physiological roles of STAT3 S727 phosphorylation in the cell cycle control. The CDK1-mediated STAT3 S727 phosphorylation at the onset of mitosis suppresses the expression of CDK inhibitors including $p21^{CIP1/WAF1}$ and $p27^{Kip1}$, which allows CDK1 to maintain its active state during the M phase. As cells exit from the M phase, the activity of CDK1 decreases as a result of cyclin B degradation, and STAT3 becomes dephosphorylated at S727, which triggers the expression of $p21^{CIP1/WAF1}$ and $p27^{Kip1}$. Increased expression of $p21^{CIP1/WAF1}$ and $p27^{Kip1}$ further inhibits CDK1 activity, forming a negative feedback loop. Furthermore, both $p21^{CIP1/WAF1}$ and $p27^{Kip1}$ are actively involved in the G1 checkpoint control at the "restriction point" by regulating CDK4/6 activities until the requirements for further proliferation are met.

The antagonistic nature of the relationship between S727 and Y705 raised the question as to whether the G1-arresting effect of S727A is mediated through the increase of Y705 phosphorylation. Attempts to express a double mutant of STAT3 that carried both S727A and Y705F mutations in HeLa cell have so far been unsuccessful. No expression of the double mutant was detected, probably due to lethal effects of the double mutation (unpublished data, Pelech et al.). However, our in vitro transcription assay with purified STAT3 WT and S727A proteins without Y705 phosphorylation indicated that the regulation of DNA-binding activity of STAT3 by S727 phosphorylation/dephosphorylation is not mediated through Y705.

In summary, our study provides the first evidence for the involvement of a STAT protein in the cell cycle regulation through its direct phosphorylation by a CDK. The CDK1-mediated STAT3 serine phosphorylation may be critical for the antitumor properties of microtubule-interfering agents. Thus, in-depth understanding of the signaling pathways leading to STAT3 serine phosphorylation shall shed more light on the mechanisms underlying the actions of microtubule-interfering agents routinely used in cancer chemotherapy to facilitate their improved efficacy.

REFERENCES

1. Levy, D. E., and Darnell, J. E., Jr. (2002) Stats: transcriptional control and biological impact, *Nat. Rev. Mol. Cell Biol. 3*, 651−662.
2. Zhong, Z., Wen, Z., and Darnell, J. E., Jr. (1994) Stat3: a STAT family member activated by tyrosine phosphorylation in response to epidermal growth factor and interleukin-6, *Science 264*, 95−98.
3. Schinder, C., Shuai, K., Prezioso, V. R., and Darnell, J. E. (1992) Interferon-dependent tyrosine phosphorylation of a latent cytoplasmic transcription factor, *Science 257*, 809−813.
4. Shuai, K., Stark, G. R., Kerr, I. M., and Darnell, J. E. (1993) A single phosphotyrosine residue of Stat91 required for gene activation by interferon-gamma, *Science 261*, 1744−1746.
5. Garcia, R., Yu, C. L., Hudnall, A., Catlett, R., Nelson, K. L., Smithgall, T., Fujita, D. J., Eithier, S. P., and Jove, R. (1997) Constitutive activation of Stat3 in fibroblasts transformed by diverse oncoproteins and in breast carcinoma cells, *Cell Growth Differ. 8*, 1267−1276.
6. Grandis, J. R., Drenning, S. D., Chakraborty, A., Zhou, M. Y., Zeng, Q., Pitt, A. S., and Tweardy, D. J. (1998) Requirement of Stat3 but not Stat1 activation for epidermal growth factor receptor-mediated cell growth In vitro, *J. Clin. Invest. 102*, 1385−1392.

7. Weber-Nordt, R. M., Egen, C., Wehinger, J., Ludwig, W., Gouilleux-Gruart, V., Mertelsmann, R., and Finke, J. (1996) Constitutive activation of STAT proteins in primary lymphoid and myeloid leukemia cells and in Epstein-Barr virus (EBV)-related lymphoma cell line, *Blood 88*, 809−816.
8. Eilers, A., Georgellis, D., Klose, B., Schindler, C., Ziemiecki, A., Harpur, A. G., Wilks, A. F., and Decker, T. (1995) Differentiation-regulated serine phosphorylation of STAT1 promotes GAF activation in macrophages, *Mol. Cell Biol. 15*, 3579−3586.
9. Wen, Z., Zhong, Z., and Darnell, J. E., Jr. (1995) Maximal activation of transcription by Stat1 and Stat3 requires both tyrosine and serine phosphorylation, *Cell 82*, 241−250.
10. Zhang, X., Blenis, J., Li, H. C., Schindler, C., and Chen-Kiang, S. (1995) Requirement of serine phosphorylation for formation of STAT-promoter complexes, *Science 267*, 1990−1994.
11. Wen, Z., and Darnell, J. E., Jr. (1997) Mapping of Stat3 serine phosphorylation to a single residue (727) and evidence that serine phosphorylation has no influence on DNA binding of Stat1 and Stat3, *Nucleic Acids Res. 25*, 2062−2067.
12. Yamashita, H., Xu, J., Erwin, R. A., Farrar, W. L., Kirken, R. A., and Rui, H. (1998) Differential control of the phosphorylation state of proline-juxtaposed serine residues Ser725 of Stat5a and Ser730 of Stat5b in prolactin-sensitive cells, *J. Biol. Chem. 273*, 30218−30224.
13. Chung, J., Uchida, E., Grammer, T. C., and Blenis, J. (1997) STAT3 serine phosphorylation by ERK-dependent and -independent pathways negatively modulates its tyrosine phosphorylation, *Mol. Cell. Biol. 17*, 6508−6516.
14. Kovarik, P., Stoiber, D., Eyers, P. A., Menghini, R., Neininger, A., Gaestel, M., Cohen, P., and Decker, T. (1999) Stress-induced phosphorylation of STAT1 at Ser727 requires p38 mitogen-activated protein kinase whereas IFN-gamma uses a different signaling pathway, *Proc. Natl. Acad. Sci. U.S.A. 96*, 13956−13961.
15. Zhang, T., Kee, WH., Seow, KH., Fung, W., and Cao, X. (2000) The coiled-coil domain of Stat3 is essential for its SH2 domain-mediated receptor binding and subsequent activation induced by epidermal growth factor and interleukin-6, *Mol. Cell. Biol. 20*, 7132−7139.
16. Jain, N., Zhang, T., Kee, W. H., Li, W., and Cao, X. (1999) Protein kinase C delta associates with and phosphorylates Stat3 in an interleukin-6-dependent manner, *J. Biol. Chem. 274*, 24392−24400.
17. Yokogami, K., Wakisaka, S., Avruch, J., and Reeves, S. A. (2000) Serine phosphorylation and maximal activation of STAT3 during CNTF signaling is mediated by the rapamycin target mTOR, *Curr Biol. 10*, 47−50.
18. Ramana, C. V., Grammatikakis, N., Chernov, M., Nguyen, H., Goh, K. C., Williams, B. R., and Stark, G. R. (2000) Regulation of c-myc expression by IFN-gamma through Stat1-dependent and -independent pathways, *EMBO J. 19*, 263−272.
19. Decker, T., and Kovarik, P. (2000) Serine phosphorylation of STATs, *Oncogene 19*, 2628−2637.
20. Wood, K. W., Cornwell, W. D., and Jackson, J. R. (2001) Past and future of the mitotic spindle as an oncology target, *Curr. Opin. Pharmacol. 1*, 370−377.
21. Zhang, H., Shi, X., Zhang, Q. J., Hampong, M., Paddon, H., Wahyuningsih, D., and Pelech, S. (2002) Nocodazole-induced p53-dependent c-Jun N-terminal kinase activation reduces apoptosis in human colon carcinoma HCT116 cells, *J. Biol. Chem. 277*, 43648−43658.
22. Zhang, H., Shi, X., Paddon, H., Hampong, M., Dai, W., and Pelech, S. (2004) B23/nucleophosmin serine 4 phosphorylation mediates mitotic functions of polo-like kinase 1, *J. Biol. Chem. 279*, 35726−35734.
23. Cao, X., Tay, A., Guy, G. R., and Tan, Y. H. (1996) Activation and association of Stat3 with Src in v-Src-transformed cell lines, *Mol. Cell. Biol. 16*, 1595−1603.
24. Pelech, S., Sutter, C., and Zhang, H. (2003) Kinetworks protein kinase multiblot analysis, *Methods Mol. Biol. 218*, 99−111.
25. Gussio, R., Zaharevitz, D. W., McGrath, C. F., Pattabiraman, N., Kellogg, G. E., Schultz, C., Link, A., Kunick, C., Leost, M., Meijer, L., and Sausville, E. A. (2000)Structure-based design modifications of the paullone molecular scaffold for cyclin-dependent kinase inhibition, *Anticancer Drug Des. 15*, 53−66.
26. Knockaert, M., Greengard, P., and Meijer, L. (2002) Pharmacological inhibitors of cyclin-dependent kinases, *Trends Pharmacol. Sci. 23*, 417−425.
27. Clark-Lewis, I., Sanghera, J. S., and Pelech, S. L. (1991) Definition of a consensus sequence for peptide substrate recognition by p44mpk, the meiosis-activated myelin basic protein kinase, *J. Biol. Chem. 266*, 15180−15184.
28. Chen, X., Oh, S. W., Zheng, Z., Chen, H. W., Shin, H. H., and Hou, S. X. (2003) Cyclin D-Cdk4 and cyclin E-Cdk2 regulate the Jak/STAT signal transduction pathway in Drosophila, *Dev. Cell 4*, 179−190.
29. Fu, A. K., Fu, W. Y., Ng, A. K., Chien, W. W., Ng, Y. P., Wang, J. H., and Ip, N. Y. (2004) Cyclin-dependent kinase 5 phosphorylates signal transducer and activator of transcription 3 and regulates its transcriptional activity, *Proc. Natl. Acad. Sci. U.S.A. 101*, 6728−6733.
30. Lew, J., Huang, Q. Q., Qi, Z., Winkfein, R. J., Aebersold, R., Hunt, T., and Wang, J. H. (1994) A brain-specific activator of cyclin-dependent kinase 5, *Nature 371*, 423−426.
31. Liang, H., Venema, V. J., Wang, X., Ju, H., Venema, R. C., and Marrero, M. B. (1999) Regulation of angiotensin II-induced phosphorylation of STAT3 in vascular smooth muscle cells, *J. Biol. Chem. 274*, 19846−19851.
32. Ng, J., and Cantrell, D. (1997) STAT3 is a serine kinase target in T lymphocytes. Interleukin 2 and T cell antigen receptor signals converge upon serine 727, *J. Biol. Chem. 272*, 24542−24549.
33. Sherr, C. J., and Roberts, J. M. (1999) CDK inhibitors: positive and negative regulators of G1-phase progression, *Genes Dev. 13*, 1501−1512.
34. Barre, B., Avril, S., and Coqueret, O. (2003) Opposite regulation of myc and p21waf1 transcription by STAT3 proteins, *J. Biol. Chem. 278*, 2990−2996.
35. Coqueret, O., and Gascan, H. (2000) Functional interaction of STAT3 transcription factor with the cell cycle inhibitor p21WAF1/CIP1/SDI1, *J. Biol. Chem. 275*, 18794−18800.
36. de Koning, J. P., Soede-Bobok, A. A., Ward, A. C., Schelen, A. M., Antonissen, C., van Leeuwen, D., Lowenberg, B., and Touw, I. P. (2000) STAT3-mediated differentiation and survival and of myeloid cells in response to granulocyte colony-stimulating factor: role for the cyclin-dependent kinase inhibitor p27(Kip1), *Oncogene 19*, 3290−3298.
37. Macleod, K. F., Sherry, N., Hannon, G., Beach, D., Tokino, T., Kinzler, K., Vogelstein, B., and Jacks, T. (1995) p53-dependent and independent expression of p21 during cell growth, differentiation, and DNA damage, *Genes Dev. 9*, 935−944.
38. Stewart, Z. A., Leach, S. D., and Pietenpol, J. A. (1999) p21-(Waf1/Cip1) inhibition of cyclin E/Cdk2 activity prevents endoreduplication after mitotic spindle disruption, *Mol. Cell. Biol. 19*, 205−215.

BI052490J